

This discussion paper is/has been under review for the journal *Atmospheric Chemistry and Physics (ACP)*. Please refer to the corresponding final paper in *ACP* if available.

Stratospheric ozone in the post-CFC era

F. Li et al.

Stratospheric ozone in the post-CFC era

F. Li¹, R. S. Stolarski², and P. A. Newman²

¹GEST, University of Maryland, Baltimore County, Baltimore, MD, USA

²Atmospheric Chemistry and Dynamics Branch, NASA GSFC, Greenbelt, MD, USA

Received: 19 September 2008 – Accepted: 22 September 2008 – Published: 3 December 2008

Correspondence to: F. Li (Feng.Li@nasa.gov)

Published by Copernicus Publications on behalf of the European Geosciences Union.

Title Page

Abstract

Introduction

Conclusions

References

Tables

Figures

◀

▶

◀

▶

Back

Close

Full Screen / Esc

Printer-friendly Version

Interactive Discussion



Abstract

Vertical and latitudinal changes in the stratospheric ozone in the post-chlorofluorocarbon (CFC) era are investigated using simulations of the recent past and the 21st century with a coupled chemistry-climate model. Model results reveal that, in the 2060s when the stratospheric halogen loading is projected to return to its 1980 values, the extratropical column ozone is significantly higher than that in 1975–1984, but the tropical column ozone does not recover to 1980 values. Upper and lower stratospheric ozone changes in the post-CFC era have very different patterns. Above 15 hPa ozone increases almost latitudinally uniformly by 6 Dobson Unit (DU), whereas below 15 hPa ozone decreases in the tropics by 8 DU and increases in the extratropics by up to 16 DU. The upper stratospheric ozone increase is a photochemical response to greenhouse gas induced strong cooling, and the lower stratospheric ozone changes are consistent with enhanced mean advective transport due to a stronger Brewer-Dobson circulation. The model results suggest that the strengthening of the Brewer-Dobson circulation plays a crucial role in ozone recovery and ozone distributions in the post-CFC era.

1 Introduction

The stratospheric ozone layer is expected to recover to pre-1980 levels in the middle of the 21st century with the projected decline of the stratospheric halogen loading (WMO, 2007). Coupled chemistry-climate model (CCM) simulations have found that the recovery of the stratospheric ozone and halogen to 1980 levels will not happen at the same time, because ozone recovery is strongly dependant on temperature and transport, which in the middle 21st century, are significant different from those in the 1980s (Eyring et al., 2007). Increased greenhouse gases (GHG) will cool the stratosphere, which will lead to an increase in ozone due to the temperature dependence of the chemical reactions involved in ozone loss (Barnett et al., 1975). Additionally,

Stratospheric ozone in the post-CFC era

F. Li et al.

Title Page

Abstract

Introduction

Conclusions

References

Tables

Figures

◀

▶

◀

▶

Back

Close

Full Screen / Esc

Printer-friendly Version

Interactive Discussion



model simulations find that the Brewer-Dobson circulation will speed up with the increase in GHGs (e.g., Butchart et al., 2006), resulting in more ozone transport to the mid-high latitudes and could advance ozone recovery in the extratropical region (Austin and Wilson, 2006).

5 An important aspect of ozone recovery is the vertical and latitudinal characteristics of the ozone distribution in the post-chlorofluorocarbon (CFC) era, which has not been investigated in detail by previous work. Changes in temperature and transport have very different effects on ozone abundance in the upper and lower stratosphere because of the ozone photochemical lifetime differences in the two regions (Shepherd, 2008). The acceleration of the Brewer-Dobson circulation will change the latitudinal distribution of ozone by bringing more ozone-poor air into the tropical lower stratosphere and more ozone-rich air into the mid-high latitudes. A detailed examination of the vertical and latitudinal structure of ozone changes will help us to understand how the ozone layer is affected by climate change.

10 This paper investigates the impacts of climate change on ozone recovery using simulations of the recent past (late 20th century) and future (21st century) from the Goddard Earth Observing System (GEOS) CCM (Pawson et al., 2008). We focus on vertical and latitudinal ozone changes after the stratospheric halogen loading returns to 1980 levels. Decadal differences in the stratospheric ozone between 2060s and 1975–1984 are examined when the halogen amounts are nearly the same during these two decades. These differences are interpreted as mainly caused by climate change and are consistent with an increased Brewer-Dobson circulation in the lower stratosphere and strong cooling in the upper stratosphere.

2 Model simulations

25 This study uses past and future climate simulations from GEOSCCM Version 1, which is based on the GEOS-4 General Circulation Model. It includes a comprehensive stratospheric chemistry scheme that is coupled with the physical processes through

Stratospheric ozone in the post-CFC era

F. Li et al.

Title Page

Abstract

Introduction

Conclusions

References

Tables

Figures

◀

▶

◀

▶

Back

Close

Full Screen / Esc

Printer-friendly Version

Interactive Discussion



the radiation code. The model has a horizontal resolution of $2^{\circ} \times 2.5^{\circ}$ and 55 vertical levels with a model top at 0.01 hPa. A detailed description of GEOSCCM Version 1 is given by Pawson et al. (2008).

A number of time-slice and time-dependent simulations of the recent past (1951–2005) and future (2001–2099) have been performed using the GEOSCCM Version 1. Model results have been evaluated and analyzed to address several different scientific questions (Eyring et al., 2006, 2007; Pawson et al., 2008; Perlwitz et al., 2008). Overall, model simulations of the recent past agree reasonably well with observations in stratospheric dynamics, transport, and ozone distribution and depletion (Eyring et al., 2006, 2007; Pawson et al., 2008).

For this study, two sets of simulations for the period 1975–2070 are used. The first set is forced with standard scenarios of greenhouse gases (GHG) and ozone-depleting substances (ODS) (Eyring et al., 2006). Sea-surface temperature and sea-ice amounts (SST) are from integrations of the NCAR Community Climate System Model. The external forcings used for the second simulation differ from those in the first one in that, 1. the halogen concentrations are fixed at 1960 levels, and 2. SST data for the late 20th century are from observations. These two sets of simulations are referred to as FREF (future reference runs) and Cl60 (fixed 1960 halogen amount simulations).

3 Model results

The WMO Scientific Assessment of Ozone Depletion report (2007) estimates that full recovery of ozone will likely occur when the Equivalent Effective Stratospheric Chlorine (EESC) returns to pre-1980 levels. EESC is a measure to quantify the effects of chlorine and bromine containing halogens on ozone depletion in the stratosphere (Newman et al., 2007). Evolution of EESC has the largest effect on ozone in the upper stratosphere and polar lower stratosphere. Figure 1 shows that EESC in these regions returns to 1980 values by the early 2060s in FREF. EESC in the tropics and mid-latitudes reach 1980 levels during the 2040s (not shown). Figure 1 also shows

Stratospheric ozone in the post-CFC era

F. Li et al.

Title Page

Abstract

Introduction

Conclusions

References

Tables

Figures

◀

▶

◀

▶

Back

Close

Full Screen / Esc

Printer-friendly Version

Interactive Discussion



**Stratospheric ozone
in the post-CFC era**

F. Li et al.

[Title Page](#)[Abstract](#)[Introduction](#)[Conclusions](#)[References](#)[Tables](#)[Figures](#)[◀](#)[▶](#)[◀](#)[▶](#)[Back](#)[Close](#)[Full Screen / Esc](#)[Printer-friendly Version](#)[Interactive Discussion](#)

that, except in the tropics, the column ozone returns to 1980 values much earlier than the EESC does. The earliest ozone recovery occurs in the Northern Hemisphere (NH) mid-latitudes and the Arctic at about 2025. Recovery of the global, Southern Hemisphere (SH) mid-latitude, and Antarctic column ozone happens between 2040–2045. In the early 2060s when the EESC returns to 1980 values, ozone amounts in these regions are higher than their 1980 values, indicating a super recovery. The tropical ozone is an exception. It is least affected by EESC with a maximum depletion of less than 3%, but it never recovers to 1980 values during the simulations.

The ozone evolution from 1980–2070 in FREF is similar to many other CCM projections (Eyring et al., 2007). The different recovery dates between ozone and EESC strongly suggest that GHG increases have a significant impact on ozone recovery. The focus of this study is the effects of climate change on the vertical and latitudinal ozone changes. In order to separate the contributions to ozone changes from ODS and GHG increase, we examine the decadal differences in ozone between 1975–1984 and 2060–2069. In FREF simulations, EESC has recovered to pre-1980 values in the 2060s. The differences in EESC between 2060–2069 and 1975–1984 are within 10% in regions that are mostly affected by ODS, i.e., the upper stratosphere and polar regions. Therefore we interpret decadal differences in the stratospheric ozone and dynamics between these two decades are mostly due to GHG increase.

Ozone changes between 2060–2069 and 1975–1984 have very different features in the upper and lower stratosphere (Fig. 2a). Above about 15 hPa, ozone concentrations increase everywhere and this increase is almost latitudinally uniform in the subpolar region. Below 15 hPa, ozone concentrations decrease in the tropics and increase in most of the extratropics. Lower stratospheric ozone changes stand out when the changes are plotted in Dobson Unit (DU)/km, showing a near hemispheric symmetric pattern (Fig. 2b). However, there are quantitative inter-hemispheric differences. For example, the bell-shaped negative region in the tropics extends further into the SH mid-latitudes and the lower stratospheric ozone increase at 60° N is larger than at 60° S.

Figure 2c shows the column ozone changes and the contributions from above and

**Stratospheric ozone
in the post-CFC era**

F. Li et al.

[Title Page](#)[Abstract](#)[Introduction](#)[Conclusions](#)[References](#)[Tables](#)[Figures](#)[◀](#)[▶](#)[◀](#)[▶](#)[Back](#)[Close](#)[Full Screen / Esc](#)[Printer-friendly Version](#)[Interactive Discussion](#)

below 15 hPa (hereafter referred as upper and lower stratosphere, respectively). Total column ozone changes are marked by increases in the extratropics and small decreases in the tropics. These differences are statistically significant except in the southern high latitudes. The largest increase occurs around 60° in both hemispheres, with peaks of 23 DU (6%) in the NH and 13 DU (3%) in the SH. The latitudinal structure of column ozone is almost solely due to changes in the lower stratosphere, where ozone decreases by 8 DU in the tropics, and increase by up to 16 and 7 DU in the northern and southern extratropics, respectively. The uniform increase of upper stratospheric ozone (~6 DU) also makes a significant contribution to the total column ozone changes, especially in the tropics and SH. Interestingly, the opposite ozone changes in the tropical and extratropical lower stratosphere nearly cancel each other, resulting in an area-weighted global-mean lower stratospheric ozone change of -0.4 DU. Therefore the global-mean total column ozone increase (5.3 DU) is attributed to increases in the upper stratospheric ozone (5.7 DU).

The very different structures in the upper and lower stratospheric ozone changes strongly indicate different ozone control mechanisms in the two regions. Intuitively, the increase in the upper stratospheric ozone suggests a chemical response to GHG cooling, whereas the unique latitudinal structure of the lower stratospheric ozone changes indicates an acceleration of the Brewer-Dobson circulation. We now examine changes in temperature and the Brewer-Dobson circulation between 2060–2069 and 1975–1984, and discuss whether these changes are consistent with the ozone changes.

Increased CO₂ results in a warming in the troposphere and cooling in the stratosphere (Fig. 2d). The cooling in the stratosphere increases with height, reaching a value of 8 K (or about 1 K/decade) near the stratopause. A reverse relationship between ozone and temperature in the upper stratosphere has long been known, which is mostly due to the strong temperature dependence of the chemical ozone loss rate in the Chapman reactions $O + O_3 \rightarrow 2O_2$ ($k \sim \exp[-2060/T]$) (Rosenfeld et al., 2002). Model results show that ozone loss due to O_x cycle in the upper stratosphere decreases by 10–20% in the 2060s compared to 1975–1984. Therefore GHG increases

lead to more ozone in the upper stratosphere.

Changes of the lower stratospheric ozone appear to support an enhanced advection. In a simplified view, the stratospheric transport consists of a mean advection by the Brewer-Dobson circulation and horizontal mixing. The horizontal mixing in CCMs is very difficult to be quantitatively diagnosed as an underlying general theory is still missing, but we can assess changes in the mean transport by examining the residual circulation. Figure 2e shows an overall accelerated Brewer-Dobson circulation in the 2060s compared with 1975–1984. In the tropics, upwelling increases from the tropopause to the stratopause. At 70 hPa between 20° S and 20° N, the magnitude of increase is 26%, or about 3% per decade, which is within the range of tropical mass flux increase reported by other modeling groups (Butchart et al., 2006). The enhanced tropical upward mass flux is balanced by an increase in the extratropical downwelling, although it should be noted that there exist regions where downwelling actually becomes weaker. Most notably these regions include the Arctic lower stratosphere (70° N–90° N, 100–10 hPa) and a narrow band centered at 60° S from 100 to about 5 hPa.

Figure 2f shows that the accelerated Brewer-Dobson circulation enhances the mean advective ozone transport $-(\bar{w}^* \frac{\partial [\bar{O}_3]}{\partial z} + \bar{v}^* \frac{\partial [\bar{O}_3]}{\partial y})$, where $[\bar{O}_3]$ is the zonal mean ozone volume mixing ratio, and \bar{v}^* and \bar{w}^* are the meridional and vertical residual velocity. Note that the actual changes of ozone advection depend on both the strength of the Brewer-Dobson circulation and the gradient of ozone. In the tropics, enhanced upwelling produces larger negative ozone tendency in the lower stratosphere and positive tendency in the upper stratosphere, because the vertical ozone gradient changes sign around 10 hPa (ozone concentrations peak around 10 hPa). In the middle and high latitudes, accelerated downwelling results in stronger negative ozone tendency in the upper stratosphere, and larger positive ozone tendency in the extratropical lower stratosphere except in a band near 60° S and the Arctic lower stratosphere.

Comparing Fig. 2f with Fig. 2b reveals that changes in ozone abundance and the mean advective ozone transport have a qualitatively similar pattern in the lower stratosphere, suggesting that lower stratospheric ozone changes are controlled mainly

**Stratospheric ozone
in the post-CFC era**

F. Li et al.

Title Page

Abstract

Introduction

Conclusions

References

Tables

Figures

◀

▶

◀

▶

Back

Close

Full Screen / Esc

Printer-friendly Version

Interactive Discussion



**Stratospheric ozone
in the post-CFC era**

F. Li et al.

[Title Page](#)[Abstract](#)[Introduction](#)[Conclusions](#)[References](#)[Tables](#)[Figures](#)[◀](#)[▶](#)[◀](#)[▶](#)[Back](#)[Close](#)[Full Screen / Esc](#)[Printer-friendly Version](#)[Interactive Discussion](#)

by changes in the mean advection. Interestingly, mean transport also shows inter-hemispheric differences in the mid-high latitudes in the lower stratosphere. It is likely that the reduced ozone advection in 50°S–70° S is responsible for a smaller SH ozone increase in this region. Note that the details of the lower stratosphere changes between the mean transport and ozone abundance are quite different. Overall, changes in ozone are smoother and have a smaller latitudinal gradient compared with changes in the mean transport. These differences are most likely due to horizontal mixing which acts to smooth tracer concentrations across latitude.

Strengthening of the Brewer-Dobson circulation is a robust response to GHG increase in model simulations (Butchart et al., 2006; Li et al., 2008). Butchart and Scaife (2001) found that an accelerated Brewer-Dobson circulation could advance ozone recovery indirectly via changes of the CFC lifetime. The direct impact of enhanced Brewer-Dobson circulation on ozone is investigated by Jiang et al. (2007) using a two-dimensional chemistry and transport model. They found that, when the 100 hPa upwelling mass flux increases by 10%, total ozone decreases by 4 DU in the tropics, and increases by 7 and 3.5 DU in the northern and southern high latitudes, respectively. The latitudinal structure and the relative magnitude of ozone changes in Jiang et al. (2007) (their Fig. 3) are in good agreement with those of the lower stratospheric ozone changes in FREF. These similarities support our argument that lower stratospheric ozone changes can be largely attributed to an enhanced mean ozone transport.

In the upper stratosphere, changes in ozone abundance and mean ozone transport have differing patterns. The mean advection shows increases in the tropics and decreases in the extratropics, whereas ozone displays a nearly latitudinal uniform increase. The opposite changes between ozone concentrations and mean advection in the extratropical upper stratosphere indicate that long-term ozone change is not determined by transport in this region, where ozone is in photochemical equilibrium (Ko et al., 1989). One may also notice that the regions of negative advection in the tropics, where mixing is weak, extend to 5 hPa (Fig. 2f), but ozone decrease is confined below

Stratospheric ozone in the post-CFC era

F. Li et al.

Title Page

Abstract

Introduction

Conclusions

References

Tables

Figures

◀

▶

◀

▶

Back

Close

Full Screen / Esc

Printer-friendly Version

Interactive Discussion



15 hPa (Fig. 2b). We think this difference suggests a shift from transport control to chemical control of ozone across 10 hPa. We estimated the lifetimes for mean ozone advection τ_{adv} and photochemical ozone loss τ_{loss} , $\tau_{\text{adv}}^{-1} = -\frac{1}{[\text{O}_3]}(\bar{w}^* \frac{\partial [\text{O}_3]}{\partial z} + \bar{v}^* \frac{\partial [\text{O}_3]}{\partial y})$ and

$\tau_{\text{loss}}^{-1} = -\bar{L}$, where \bar{L} is the zonal mean ozone loss rate. The chemical loss lifetime decreases very sharply with height. In the tropics (20° S–20° N), the chemical loss lifetime is more than 100 times longer than the advective lifetime at 70 hPa, and becomes comparable to the advective lifetime at 20 and 30 hPa (100–200 days), and is 10 times shorter than the advective timescale at 10 hPa. Because of the longer advective timescale compared with the ozone photochemical lifetime above 10 hPa, strengthening of the Brewer-Dobson circulation has little effect on the upper stratospheric ozone.

Another approach to demonstrate ozone changes caused by GHG increase is to use the Cl60 simulation in which the halogen loading is fixed at 1960 levels. Differences between 2060s and 1975–1984 in Cl60 must be caused by climate change. The decadal differences in the stratospheric ozone, temperature, and mean transport between 2060–2069 and 1975–1984 in Cl60 are qualitatively very similar to those in FREF. Figure 3 displays these Cl60 decadal differences, and shows that FREF differences (Fig. 2) are very well reproduced in Cl60. These similarities include: small decrease in the tropical total ozone, significant increase in the extratropical ozone with a larger peak value in the NH than in the SH, almost uniformly 6 DU upper stratospheric ozone increase, enhanced tropical upwelling, and increased extratropical downwelling (except in the Arctic lower stratosphere and a band around 60° S). The most notable difference between Figs. 2 and 3 is that Cl60 has a larger ozone increase in the Arctic lower stratosphere (Fig. 3c), which appears to be caused by a stronger downwelling in the NH in Cl60 (Fig. 3e and 3f). There are other quantitative differences between Figs. 2 and 3, which are likely caused by different SSTs used in simulation of the recent past, difference in EESC, and model internal variability. The overall qualitative agreement between Cl60 and FREF results, however, strongly support our interpretations of Fig. 2 as mostly attributed to climate change.

4 Discussion and conclusions

The GEOSCCM simulates EESC recovery to 1980 values in the 2060s. The decadal differences in the stratospheric ozone and dynamics between 2060–2069 and 1975–1984 are investigated to study how climate change affects the vertical and latitudinal ozone distributions. Model results reveal that the extratropical column ozone increases by up to 6% in the NH, but the tropical column ozone remains about the same, albeit smaller, after the recovery of EESC. Ozone changes have very different latitudinal structure in the upper and lower stratosphere. The latitudinally uniform increase of 6 DU in the upper stratospheric ozone is attribute to GHG-induced cooling that slows the ozone loss reactions. In the lower stratosphere, enhanced ozone advection due to a stronger Brewer-Dobson circulation results in decreases in the tropical ozone and increases in the extratropical ozone. Comparison with fixed halogen experiment supports our interpretations that these differences can be largely attributed to GHG increase.

Many CCMs have predicted that extratropical column ozone will be higher than 1980 values when EESC return to pre-1980 levels (Eyring et al., 2007). Previous work has attributed the extratropical ozone “super recovery” to increase in the middle to upper stratospheric ozone due to GHG-induced stratospheric cooling (Eyring et al., 2007). Here we show that, in the GEOSCCM simulations when EESC returns to pre-1980 levels, lower stratospheric ozone increases make significant contribution to the “super recovery” of the extratropical total ozone. In the NH extratropics, increases in the lower stratospheric ozone exceed those in the middle to upper stratosphere. Model results also project that the tropical total column ozone will not recover to 1980 values. In the tropics, the two major mechanisms through which climate change affect the stratospheric ozone, upper stratospheric cooling and strengthening of the Brewer-Dobson circulation, have opposite effects on ozone abundance. The tropical lower stratospheric ozone decrease outweighs the upper stratospheric ozone increase. These results suggest that circulation changes play a larger role in ozone recovery than previously thought.

Title Page

Abstract

Introduction

Conclusions

References

Tables

Figures

◀

▶

◀

▶

Back

Close

Full Screen / Esc

Printer-friendly Version

Interactive Discussion



**Stratospheric ozone
in the post-CFC era**

F. Li et al.

[Title Page](#)[Abstract](#)[Introduction](#)[Conclusions](#)[References](#)[Tables](#)[Figures](#)[◀](#)[▶](#)[◀](#)[▶](#)[Back](#)[Close](#)[Full Screen / Esc](#)[Printer-friendly Version](#)[Interactive Discussion](#)

The model simulated mean ozone transport changes are qualitatively consistent with the lower stratospheric ozone changes, suggesting that changes of ozone advection play a crucial role in ozone recovery. One interesting finding in this study is the inter-hemispheric differences in the changes of the Brewer-Dobson circulation and ozone advection. A close inspection of Fig. 2e-f reveals that the reduced downwelling and ozone advection at 60° S in the lower stratosphere appears to be caused by, at least partly, an equatorward shift of the locations of the maximum downwelling. This equatorward shift is associated with a narrowing of the tropical upwelling region. At 70 hPa, the turnaround latitudes (where the residual vertical velocity changes sign) in 2060–2069 are located 2 degrees equatorward of those in 1975–1984. It is not clear what causes the narrowing of the tropical upwelling. Whether these features are produced in other model simulations remains to be verified.

Acknowledgements. This research was supported by NASA's MAP program.

References

- Austin, J. and Wilson, R. J.: Ensemble simulations of the decline and recovery of stratospheric ozone, *J. Geophys. Res.*, 111, D16314, doi:10.1029/2005JD006907, 2006.
- Barnett, J. J., Houghton, J. T., and Pyle, J. A.: The temperature dependence of the ozone concentration near the stratopause, *Q. J. Roy. Meteor. Soc.*, 101, 245–257, 1975.
- Butchart, N. and Scaife, A. A.: Removal of chlorofluorocarbons by increased mass exchange between the stratosphere and troposphere in a changing climate, *Nature*, 410, 799–802, 2001.
- Butchart, N., Scaife, A. A., Bourqui, M., de Grandpré, J., Hare, S. H. E., Kettleborough, J., Langematz, U., Manzini, E., Sassi, F., Shibata, K., Shindell, D., and Sigmond, M.: Simulations of anthropogenic change in the strength of the Brewer-Dobson circulation, *Clim. Dynam.*, 27, 727–741, 2006.
- Eyring, V., Butchart, N., Waugh, D. W., et al.: Assessment of temperature, trace species, and ozone in chemistry-climate model simulations of the recent past, *J. Geophys. Res.*, 111, D22308, doi:10.1029/2006JD007327, 2006.

**Stratospheric ozone
in the post-CFC era**

F. Li et al.

[Title Page](#)[Abstract](#)[Introduction](#)[Conclusions](#)[References](#)[Tables](#)[Figures](#)[I◀](#)[▶I](#)[◀](#)[▶](#)[Back](#)[Close](#)[Full Screen / Esc](#)[Printer-friendly Version](#)[Interactive Discussion](#)

- Eyring, V., Waugh, D. W., Bodeker, G. E., Cordero, E., et al.: Multimodel projections of stratospheric ozone in the 21st century, *J. Geophys. Res.*, 112, D16303, doi:10.1029/2006JD008332, 2007.
- Jiang X., Eichelberger, S. J., Hartmann, D. L., Shia, R., and Yuan, Y. L.: Influence of doubled CO₂ on ozone via changes in the Brewer-Dobson circulation, *J. Atmos. Sci.*, 64, 2751–2755, 2007.
- Ko, M. K. W., Sze, N., and Weisenstein, D. K.: The roles of dynamical and chemical processes in determining the stratospheric concentration of ozone in one-dimensional and two-dimensional models, *J. Geophys. Res.*, 94, 9889–9896, 1989.
- Li, F., Austin, J., and Wilson, J.: The strength of the Brewer-Dobson circulation in a changing climate: coupled chemistry-climate model simulations, *J. Climate*, 21, 40–57, 2008.
- Newman, P. A., Daniel, J. S., Waugh, D. W., and Nash, E. R.: A new formulation of equivalent effective stratospheric chlorine (EESC), *Atmos. Chem. Phys.*, 7, 4537–4552, 2007, <http://www.atmos-chem-phys.net/7/4537/2007/>.
- Pawson, S., Stolarski, R. S., Douglass, A. R., Newman, P. A., Nielsen, J. E., Frith, S. M., and Gupta, M. L.: Goddard Earth Observing System chemistry-climate model simulations of stratosphere ozone-temperature coupling between 1950 and 2005, *J. Geophys. Res.*, 113, D12103, doi:10.1029/2007JD009511, 2008.
- Rosenfield, J. E., Douglass, A. R., and Considine, D. B.: The impact of increasing carbon dioxide on ozone recovery, *J. Geophys. Res.*, 107(D6), 4049, doi:10.1029/2001JD000824, 2002.
- Rosenfield, J. E. and Schoeberl, M. R.: Recovery of the tropical lower stratospheric ozone layer, *Geophys. Res. Lett.*, 32, L21806, doi:10.1029/2005GL023626, 2005.
- Shepherd, T.: Dynamics, stratospheric ozone, and climate change, *Atmos. Ocean*, 46, 117–138, 2008.
- World Meteorological Organization (WMO)/United Nations Environment Programme (UNEP): Scientific Assessment of Ozone Depletion: 2006, World Meteorological Organization, Global Ozone Research and Monitoring Project, Report No. 50, Geneva, Switzerland, 2007.

Stratospheric ozone
in the post-CFC era

F. Li et al.

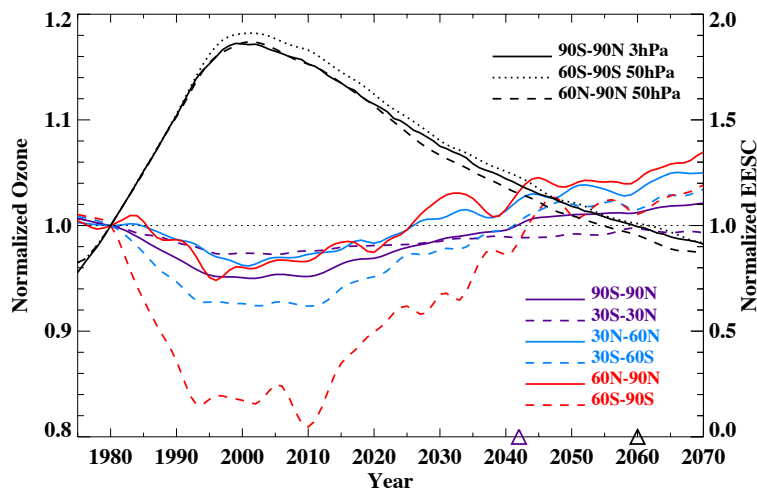


Fig. 1. Evolution of normalized annual mean EESC (black lines, right axis) and column ozone (color lines, left axis) in different regions. EESC and column ozone are normalized relative to their 1980 values. The curves are smoothed using a Gaussian filter with a half amplitude response at 8.5 years. The purple and black triangles indicate the dates of recovery of global mean column ozone and 3 hPa EESC to 1980 values, respectively.

[Title Page](#)[Abstract](#)[Introduction](#)[Conclusions](#)[References](#)[Tables](#)[Figures](#)[I◀](#)[▶I](#)[◀](#)[▶](#)[Back](#)[Close](#)[Full Screen / Esc](#)[Printer-friendly Version](#)[Interactive Discussion](#)

Stratospheric ozone
in the post-CFC era

F. Li et al.

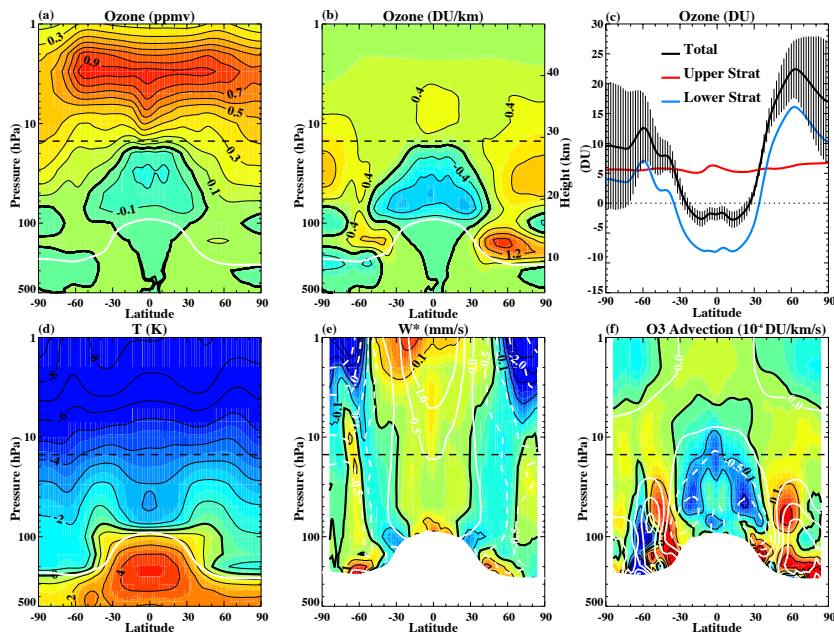


Fig. 2. Decadal differences between 2060–2069 and 1975–1984 from FREF. **(a)** Ozone concentrations in ppmv (contour interval: 0.1 ppmv). **(b)** Ozone concentrations in DU/km (contour interval: 0.4 DU/km). **(c)** Total column ozone and contributions from the upper (above 15 hPa) and lower (below 15 hPa) stratosphere. The black vertical lines indicate 2σ uncertainties of the decadal difference in the total column ozone. **(d)** Temperature (contour interval: 1 K). **(e)** The vertical residual velocity \bar{w}^* (contour interval: 0.1 mm/s). The white contours are 1975–1984 mean (contour interval: 0.5 mm/s). **(f)** The mean ozone advection $-(\bar{w}^* \frac{\partial [\bar{O}_3]}{\partial z} + \bar{v}^* \frac{\partial [\bar{O}_3]}{\partial y})$ (contour interval: 0.1×10^{-6} DU/km/s). The white contours are 1975–1984 mean (contour interval: 0.5×10^{-6} DU/km/s). The white lines in panels (a), (b) and (d) are decadal mean tropopause for 1975–1984. Panels (e) and (f) only show changes in the stratosphere.

Title Page

Abstract

Introduction

Conclusions

References

Tables

Figures

◀

▶

◀

▶

Back

Close

Full Screen / Esc

Printer-friendly Version

Interactive Discussion



Stratospheric ozone
in the post-CFC era

F. Li et al.

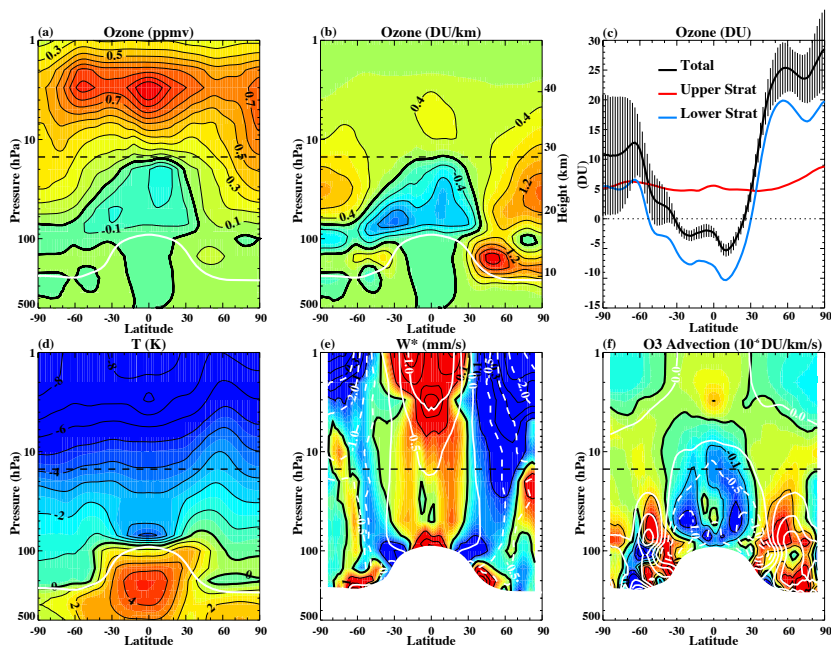


Fig. 3. Same as Fig. 2, but for simulation CI60.

[Title Page](#)[Abstract](#)[Introduction](#)[Conclusions](#)[References](#)[Tables](#)[Figures](#)[◀](#)[▶](#)[◀](#)[▶](#)[Back](#)[Close](#)[Full Screen / Esc](#)[Printer-friendly Version](#)[Interactive Discussion](#)